Article

Discovery Medicine 2025; 37(193): 326–334
https://doi.org/10.24976/Discov.Med.202537193.26

GNPNAT1 Regulation: A Key Role in Radioimmune Function and NK Cell Resistance in NSCLC

Fei Xiang[1], Yuanfei Dai[1], Chunfei Yao[1], Ying Li[1], Wei Zhao[1], Jie Wei[1,*]

[1]Department of Oncology, The Affiliated Chuzhou Hospital of Anhui Medical University (The First People's Hospital of Chuzhou), 239000 Chuzhou, Anhui, China

*Correspondence: jieweiah@163.com (Jie Wei)

Published: 20 February 2025

Background: Glucosamine-6-phosphate N-acetyltransferase 1 (GNPNAT1) is an enzyme involved in the hexosamine biosynthetic pathway, which is critical for glycosylation processes. In the context of non-small cell lung cancer (NSCLC), GNPNAT1 plays a significant role in modulating immune responses. The purpose of this study is to investigate the role of GNPNAT1 in regulating the efficacy of radiotherapy and resistance to natural killer (NK) cell-mediated cytotoxicity in patients with NSCLC.

Methods: To assess GNPNAT1's impact on radiotherapy efficacy, 122 lung cancer patients were categorized into radiosensitive and radioresistant groups. GNPNAT1 expression levels in cancerous tissues from both groups were measured using quantitative reverse transcription polymerase chain reaction (qRT-PCR) and Western blotting. This analysis was extended to various lung cancer cell lines (BEAS-2B, A549, LTEP-2, SPCA1, and H157) using the same molecular techniques. To investigate GNPNAT1's functional role in radioresistance, radioresistant A549 cells (A549R26-1) were established, and GNPNAT1 expression was genetically manipulated. Experimental groups included control, si-NC, si-GNPNAT1, Oe-NC, and Oe-GNPNAT1. Post-treatment, GNPNAT1 levels were measured via qRT-PCR and Western blotting. Cells were exposed to varying doses of radiation, and subsequent assessments included cell proliferation (Cell Counting Kit-8 (CCK-8) assay), radiosensitivity (plate cloning assays), and apoptosis rates (flow cytometry). Isolated and purified primary NK cells were co-cultured with lung cancer cells from each experimental group. The cytotoxicity of NK cells against lung cancer cells was assessed through lactate dehydrogenase (LDH) release and colony formation assays.

Results: Compared to the radiosensitive group, the radioresistant group exhibited significantly elevated GNPNAT1 expression levels ($p < 0.05$). The radioresistant cell line A549R26-1 demonstrated higher proliferation ability and lower apoptosis levels compared to its parental cell line, A549P. Subsequently, down-regulation of GNPNAT1 expression in A549R26-1 cells resulted in reduced proliferation, increased apoptosis, and weakened resistance to NK cell cytotoxicity. Conversely, up-regulation of GNPNAT1 expression in A549R26-1 cells following co-culture with NK cells led to increased proliferation and survival rates, and enhanced resistance to NK cell cytotoxicity. Notably, GNPNAT1 knockdown effectively attenuated the radioresistance of A549R26-1 cells.

Conclusion: Down-regulation of GNPNAT1 expression reduces the immune resistance of non-small cell lung cancer to radiotherapy and enhances susceptibility to NK cell cytotoxicity.

Keywords: GNPNAT1; NSCLC; radiation immunity; NK cells

Introduction

Non-small cell lung cancer (NSCLC) represents a prominent subtype of lung cancer, with treatment strategies undergoing continuous evolution [1,2]. While radiotherapy serves as a prevalent treatment modality for NSCLC patients, its efficacy is often influenced by the intricacies of the tumor microenvironment, including immune evasion mechanisms [3]. The emergence of immunotherapy in recent years has offered newfound optimism for NSCLC treatment. However, its efficacy in certain patients remains suboptimal, likely due in part to the presence of immunosuppressive factors within the tumor microenvironment [4,5]. Hence, investigating the mechanisms underlying radioimmune function and natural killer (NK) cell toxicity resistance in NSCLC holds paramount importance. Such endeavors aim to refine treatment protocols and enhance patient survival rates [6,7].

Immune checkpoint inhibitors (ICIs) have become integral to NSCLC treatment; however, not all patients derive benefit from this therapy. Studies indicate that the efficacy of immunotherapy may hinge on the regulation of various genes within tumor cells, including the immune-related gene Glucosamine-6-phosphate N-acetyltransferase 1 (GNPNAT1) [8,9]. As a pivotal metabolic regulator, GNPNAT1 potentially exerts a profound influence on immune cell activity within the tumor microenvironment [10]. GNPNAT1 plays a key role in regulating cellular sphingo-

sine metabolic pathways and may affect immune cell activity and NK cytotoxicity in the tumor microenvironment. Studies have shown that GNPNAT1 is crucial in regulating the sphingosine levels of tumor cells, and changes in sphingosine levels may impact the immune escape ability of tumor cells and their sensitivity to NK cells [11,12].

By further studying the regulatory mechanism of GNPNAT1 in NSCLC, we can better understand the impact of the tumor microenvironment on immunotherapy and provide important clues for developing new therapeutic strategies. For example, targeting GNPNAT1 may enhance the efficacy of immunotherapy and improve patient outcomes. This could include developing targeted drugs against GNPNAT1 or combining existing immunotherapies with GNPNAT1 modulators for optimal therapeutic effects. However, the specific mechanisms underlying GNPNAT1's impact on immune function and NK cell toxicity resistance in NSCLC radiotherapy remain poorly understood. Therefore, this study aims to unravel GNPNAT1's regulatory role in immune function during NSCLC radiotherapy and elucidate its mechanism concerning NK cell toxicity. By doing so, we aim to provide theoretical insights and experimental foundations for advancing novel treatment strategies [13,14].

Materials and Methods

Subject of Study

From January 2018 to January 2023, Gansu Cancer Hospital conducted a study involving 122 NSCLC patients, comprising 72 males and 50 females, aged between 40 and 67 years. The inclusion criteria were histologically confirmed NSCLC, no prior radiotherapy or chemotherapy, an Eastern Cooperative Oncology Group (ECOG) performance status of 0–2, and provision of informed consent. Exclusion criteria included the presence of other malignancies, severe comorbidities, prior thoracic surgery, and refusal to provide informed consent. The cohort consisted of 63 cases of squamous cell carcinoma and 59 cases of adenocarcinoma. All participants provided informed consent and underwent pathological examination of both tumor and adjacent tissues.

Following surgery, patients underwent three-dimensional conformal radiotherapy, receiving 2 Gray per fraction, five times a week, for a total dose ranging from 50 to 70 Gray (Gy) over 8 weeks. Radiotherapy response was evaluated based on World Health Organization (WHO) criteria [15], with patients classified as having complete response (CR), partial response (PR), progressive disease (PD), or stable disease (SD). CR and PR were considered radiosensitive outcomes, while PD and SD were considered radioresistant. Among the patients, 36 were identified as radioresistant, while 86 exhibited radiosensitivity.

GNPNAT1 expression levels in tumor tissues were assessed using Western blotting (WB) and polymerase chain reaction (PCR) techniques to identify any discrepancies.

Cell Culture

BEAS-2B (CC-Y1066), A549 (CC-Y6015), H157 (CC-Y1373), LTEP-2 (xb-qy170), and SPCA1 (FS-A9297) cell lines, acquired from ATCC (Manassas, VA, USA), were cultured in Roswell Park Memorial Institute-1640 (RPMI-1640) at 37 °C in a 5% CO_2 humidified environment. All the cells used in the experiments were identified by short tandem repeat (STR) and tested for mycoplasma contamination, with no mycoplasma infection found. All procedures followed aseptic techniques to prevent contamination.

Western Blot

Tissue and cellular proteins were extracted using established protocols, and their concentrations were determined using the bicinchoninic acid (BCA) method. Protein samples were adjusted to a loading volume of 30 µg with deionized water. Separation and concentration gels (10% SDS, 15553027, Thermo Fisher Scientific, Shanghai, China) were prepared, and protein samples were mixed with sampling buffer (ab170197, Abcam, Cambridge, UK), followed by boiling at 100 °C for 5 minutes. After cooling on ice and centrifugation, equal amounts of protein were loaded onto the gel for electrophoresis separation and then transferred to a nitrocellulose membrane. The membrane was blocked with 5% skim milk powder overnight at 4 °C. Primary antibodies targeting GNPNAT1 (1:1000, ab127697, Abcam, Cambridge, UK) and glyceraldehyde 3-phosphate dehydrogenase (GAPDH) (1:2000, ab8245, Abcam, Cambridge, UK) were applied and incubated at room temperature for 1 hour. Following Phosphate Buffered Saline (PBS, 10010023, Thermo Fisher Scientific) washing, secondary antibodies (1:10,000, ab205718, ab205719, Abcam, Cambridge, UK) were added and incubated for 1 hour at room temperature. After additional PBS washes, the membrane was incubated in enhanced chemiluminescence (ECL) reaction solution (Pierce, USA) for 1 minute at room temperature. Excess liquid was removed, and the membrane was covered with plastic wrap before X-ray imaging to visualize the results. GAPDH served as the internal reference, and the relative expression level of the protein was determined by calculating the ratio of the target band's gray value to that of the internal reference band.

Quantitative Reverse Transcription Polymerase Chain Reaction (qRT-PCR)

Tissue and cellular RNA were extracted using the Trizol kit (15596026, Thermo Fisher Scientific) following the manufacturer's instructions. Subsequently, the extracted RNA was reverse-transcribed into complementary DNA (cDNA) using the RevertAid First Strand cDNA Synthesis Kit (9007-49-2, Thermo Fisher Scientific). GNPNAT1 expression levels were assessed using the SYBR Premix Ex Taq II Kit (740701, Takara Bio Inc., Shiga, Japan). β-actin served as the internal reference for GNPNAT1, with primer

Table 1. Primer sequences.

Gene	Direction	Sequence (5′-3′)
GNPNAT1	F	ACTCCTATGTTTGACCCAAGTCT
	R	TCTGTTAGCTGACCCAATACCT
β-actin	F	AGCAAGCAGGAGTATGACGAGT
	R	CGTACAGGTCTTTGCGGATGT

F, forward; R, reverse; *GNPNAT1*, Glucosamine-6-phosphate N-acetyltransferase 1.

sequences detailed in Table 1. The relative expression of each target gene was determined using the $2^{-\Delta\Delta Ct}$ method, with all experiments performed in triplicate.

Radioresistant Cell Lines

A549P cells underwent weekly irradiation ranging from 2 to 6 Gy over 4 to 5 weeks. Following the resumption of cell growth post-irradiation, additional weekly radiotherapy sessions were administered. Upon reaching a cumulative dose of 26 Gy, the cells were designated as A549P/A549R26-1 cells.

Cell Transfection

A549R26-1 cells from the P5 passage, during the logarithmic growth phase, were seeded in 24-well plates at a density of 5×10^4 cells per well. Upon reaching 80% confluence, transfection was performed using the Lipofectamine™ 2000 kit (11668019, Invitrogen, Carlsbad, CA, USA) following the manufacturer's instructions. The transfection mixture was prepared by diluting the transfection sequence in 250 µL RPMI 1640 medium without serum and incubating for 5 minutes. Simultaneously, 250 µL RPMI 1640 medium without serum was mixed with 5 µL Lipofectamine™ 2000 and incubated for 5 minutes. The two solutions were then combined and further incubated for 20 minutes before addition to the cell culture wells, along with 2 µg of pcDNA2.5 plasmid vector containing the desired genetic material. After a 6-hour incubation at 37 °C with 5% CO_2 and saturated humidity, the transfection medium was replaced with RPMI 1640 medium containing 10% fetal bovine serum for subsequent experiments. The cells were divided into 9 groups: Blank group (untreated cells), Oe-NC group (cells transfected with GNPNAT1 high expression plasmid negative control), Oe-GNPNAT1 group (cells transfected with GNPNAT1 high expression plasmid), si-NC group (cells transfected with GNPNAT1 silencing negative control, sequence: 5′-ACGUGACACGUUCGGAGAA-3′), and si-GNPNAT1 group (cells transfected with GNPNAT1 silencing, sequence: 5′-CCUUGAAUGUCUACCACAATT-3′).

Cell Counting Kit-8 (CCK-8)

Cells from each group were seeded into 96-well plates with 100 µL of 1×10^4 cells per well. After a 12-hour incubation at 37 °C, the cells were irradiated with varying doses (0, 2, 4, 6, and 8 Gy) using a Cs-137 source with a dose rate ranging from 180-205 cGy/min. After 72 hours, cell proliferation was assessed by adding 10 µL of CCK-8 reagent (C0037, Biyuntian Biotechnology Co., Ltd., Shanghai, China) to each well and incubating at 37 °C for 2 hours. Absorbance was measured at 450 nm/630 nm using a microplate reader (Model Multiskan FC, Thermo Fisher Scientific). Each group consisted of three replicate wells, and the average value was calculated. The experiment was performed in triplicate.

Plate Cloning

Transfected cells from each experimental group were detached using trypsin and suspended to generate a cell suspension. The suspension was appropriately diluted and plated into 10 cm cell culture dishes at a density of 1000 cells per dish. Following a 12-hour incubation period, the cells were irradiated with varying doses (0, 2, 4, 6, and 8 Gy) from a Cs-137 source with a dose rate ranging from 180–205 cGy/min. After incubating for 10 days, the cells were fixed with methanol and stained with a 0.5% crystal violet solution. Clones containing more than 50 cells were counted visually, and the number of cell clones within each dish was recorded. Subsequently, the surviving fraction (SF) was calculated using the formula: (experimental group plating efficiency (PE)/control group PE) × 100%.

Flow Cytometry

Cells from each experimental group were seeded into 6-well plates at a density of 1000 cells per well in 1 mL of cell medium. After a 12-hour incubation period at 37 °C, the cells were exposed to various doses (0, 2, 4, 6, and 8 Gy) of radiation from a Cs-137 source, with a dose rate ranging from 180–205 cGy/min. After 48 hours of culture, the cells were detached using trypsin without Ethylenediaminetetraacetic acid (EDTA) and collected into flow tubes. The supernatant was removed by centrifugation, and the cells were washed three times with cold PBS. Subsequently, the cells were resuspended in Annexin-V- fluorescein isothiocyanate/propidium iodide (FITC/PI) staining solution (Biyuntian Biotechnology Co., Ltd., Shanghai, China) following the manufacturer's instructions. The staining solution, with 1×10^6 cells per 100 µL, was incubated at room temperature for 15 minutes. Afterward, 1 mL of 4-(2-hydroxyethyl)-1-piperazineethanesulfonic acid (HEPES) buffer solution (PPB020, Sigma-Aldrich, Shanghai, China) was added, and the mixture was gently mixed. Fluorescence emissions for FITC and PI were measured using excitation wavelengths of 488 nm, with bandpass filters at 525 nm and 620 nm, respectively. The cell apoptosis rate was determined based on the distribution of cells across four quadrants: upper left (necrotic cells), upper right (late apoptotic cells), lower right (early apoptotic cells), and lower left (viable cells). The apoptosis rate was calculated as [(early

apoptotic cells + late apoptotic cells)/total number of cells] $\times$ 100%. Triplicate assessments were performed for each experimental group.

Isolation and Detection of NK Cells

Naive natural killer (NK) cells were isolated from healthy donors' peripheral blood mononuclear cells (PBMCs) using a specialized NK cell isolation kit (071E208.11, Miltenyi Biotec, Shanghai, China). Following isolation, the cells were cultured in a dedicated NK cell medium enriched with interleukin-2 (IL-2). The purity of the isolated NK cells, identified by their CD56 + CD3- phenotype, was assessed via flow cytometry after staining with anti-CD56-PE (A23369, ABclonal, Wuhan, China,) and anti-CD3-FITC (981002, BioLegend, CA, USA) antibodies. Subsequently, the NK cells were cultured in alpha minimal essential medium (α-MEM) medium supplemented with essential nutrients such as sodium bicarbonate, inositol, 2-mercaptoethanol, and folic acid, along with horse serum and fetal calf serum to support optimal cell growth and function. This comprehensive culture approach ensured the viability and functionality of the NK cells for subsequent experimental analyses.

The Cytotoxicity of NK Cells was Determined by Colony Formation Assay

In each experimental group, 3000 lung cancer cells were seeded onto a 10 cm cell culture dish. The following day, NK cells (15,000 cells per group) were added for co-culture. After a 4-hour co-culture period, the NK cells were removed, and a fresh medium was added to the tumor cells. Colony formation was assessed after 10 days of culture using crystal violet staining, and colonies were counted under a microscope. Cell survival was quantified by comparing the ratio of colony formation observed in the experimental group to that of the control group. This approach enabled the evaluation of NK cell-mediated cytotoxicity on lung cancer cell survival across various effector-to-target cell ratios.

The Cytotoxicity of NK Cells was Analyzed by Lactate Dehydrogenase (LDH) Release Assay

To assess the cytotoxic activity of NK cells against each experimental group, lung cancer cells (3000 cells per group) were initially seeded into 10 cm cell culture dishes. Following overnight incubation, NK cells (15,000 cells per group) were added the next day. After a 4-hour co-incubation period, cytotoxicity was measured using the LDH Cytotoxicity Assay Kit (299-50601, Thermo Fisher Scientific) in 50 µL of media. Adjustments were made for spontaneous release from effector cells at the corresponding dilution to account for baseline levels. Cytotoxicity was calculated using the formula: (experimental value – effector cell spontaneous control – target cell spontaneous control)/(maximum target cell control – target cell spontaneous control) $\times$ 100%.

Data Analysis

Statistical analysis was performed using SPSS 21.0 software (SPSS, Inc., Chicago, IL, USA). The normality of data distribution was assessed using the Kolmogorov-Smirnov test. Mean values with their respective standard deviations were calculated to summarize the results. To compare multiple groups, One-Way ANOVA was applied, followed by Fisher's least significant difference *t*-test (LSD-*t*) for post-hoc pairwise comparisons. Count data were presented as rates or percentages and analyzed using the chi-square test. Statistical significance was defined as a two-sided *p*-value less than 0.05. This systematic approach ensured comprehensive and reliable analysis of the experimental data.

Results

GNPNAT1 Expression in Lung Cancer Tissues and Purity of NK Cells Extracted from Healthy Blood

To investigate GNPNAT1's role in lung cancer radioresistance, patients were classified into radioresistant and radiosensitive groups based on their response to radiotherapy. GNPNAT1 expression levels in cancer tissues from both groups were assessed using qRT-PCR and Western blot analysis. Results indicated significant upregulation of GNPNAT1 expression in the radioresistant group compared to the radiosensitive group (Fig. 1A,B, $p < 0.05$). Additionally, NK cells were purified from healthy donor PBMCs using the NK Cell Isolation Kit, with NK cell purity confirmed to be 92.56 $\pm$ 7.44%, consistent with the characteristic NK cell phenotype (Fig. 1C).

GNPNAT1 was Expressed in Lung Cancer Cells

To identify cells with the most significant differences, we compared GNPNAT1 expression in lung cancer cell lines with BEAS-2B cells. Compared to BEAS-2B cells, A549, LTEP-2, SPCA1, and H157 cells showed significantly increased GNPNAT1 expression as determined by Western blot and qRT-PCR (Fig. 2A,B, $p < 0.05$). Specifically, A549 cells exhibited the greatest difference compared to BEAS-2B cells.

Radioresistance of Radioresistant Lung Cancer Cells and Parental Cells

To investigate the impact of radioresistance on cell behavior, both A549R26-1 and parental A549 cell lines were subjected to CCK-8 assay and colony formation assay to assess their proliferation and survival rates. The results demonstrated that A549R26-1 cells exhibited enhanced proliferation and survival rates compared to A549 cells (Fig. 3A,B, $p < 0.05$). Additionally, flow cytometry analysis revealed a lower apoptosis rate in A549R26-1 cells compared to A549 cells (Fig. 3C, $p < 0.05$). These findings suggest that radioresistant lung cancer cells exhibit greater resistance to radiation compared to their parental counter-

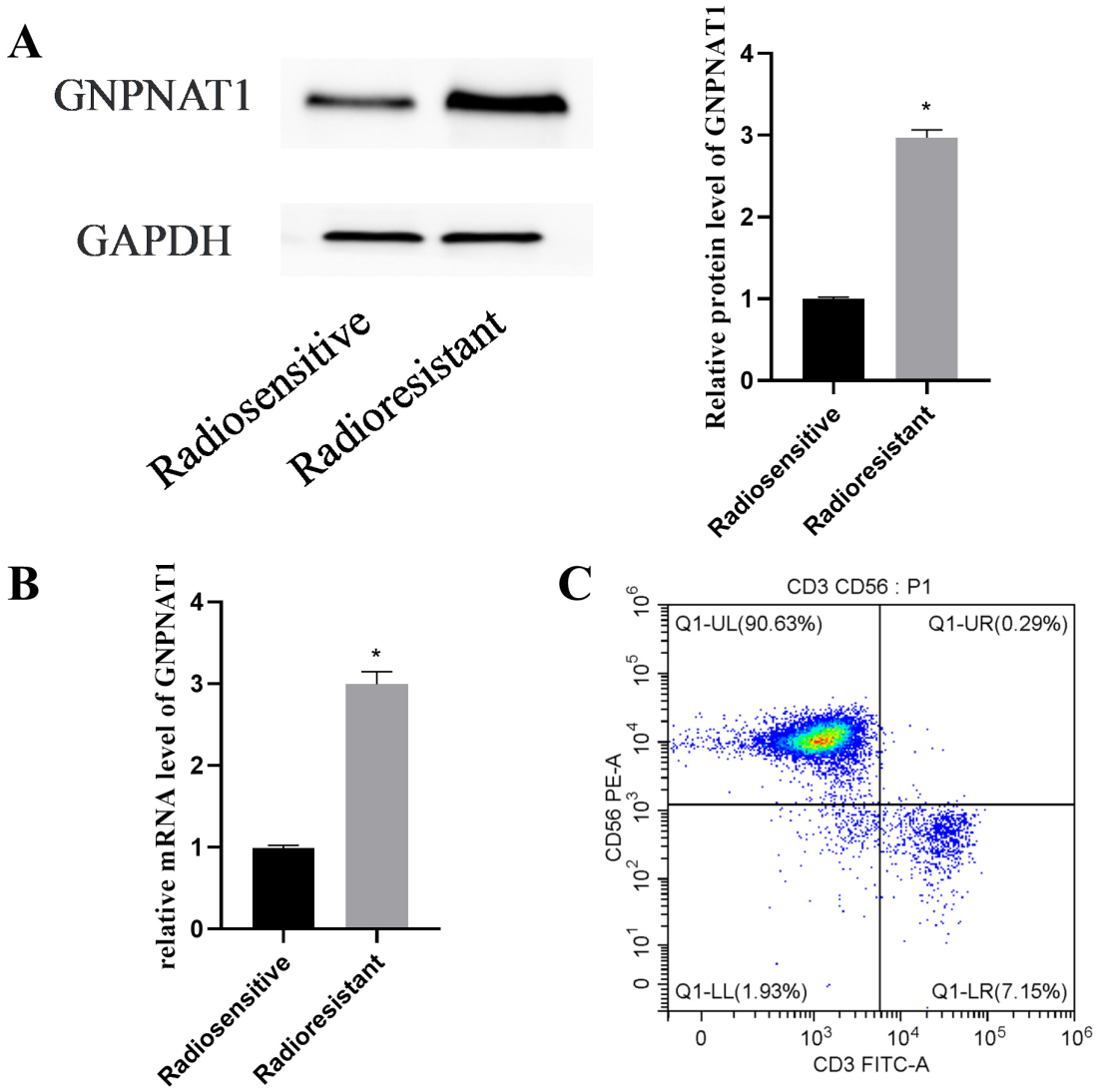

Fig. 1. GNPNAT1 expression in lung cancer tissues and purity of NK cells extracted from healthy blood. (A) Western blot detection of GNPNAT1 protein expression. (B) Quantitative reverse transcription polymerase chain reaction (qRT-PCR) detection of GNPNAT1 expression. (C) Purity of NK cells by flow cytometry: 92.56 ± 7.44%. * $p < 0.05$. n = 122 (radioresistant = 36, radiosensitivity = 86). GAPDH, glyceraldehyde 3-phosphate dehydrogenase; NK, natural killer.

parts.

Effect of GNPNAT1 on Radioresistance of Anti-Radiation Lung Cancer Cells

qRT-PCR and Western blot analyses were used to assess GNPNAT1 expression levels in A549R26-1 cells. Compared to the si-NC group, the si-GNPNAT1 group exhibited decreased GNPNAT1 expression, while the oe-GNPNAT1 group showed increased expression compared to the oe-NC group, indicating successful modulation of GNPNAT1 levels in A549R26-1 cells (Fig. 4A,B, $p < 0.05$).

To investigate the radiosensitivity of A549R26-1 cells with different GNPNAT1 expression levels, a plate cloning assay was conducted to determine cell survival rates. The cell proliferation and survival rates were lower in the si-GNPNAT1 group compared to the si-NC group, and higher in the oe-GNPNAT1 group compared to the oe-NC group (Fig. 4C, $p < 0.05$).

Flow cytometry results showed that the apoptosis rate was higher in the si-GNPNAT1 group compared to the si-NC group. Conversely, compared to the oe-NC group, the apoptosis rate was decreased in the oe-GNPNAT1 group. These findings collectively suggest that downregulation of GNPNAT1 diminishes radioresistance in lung cancer cells (Fig. 4D, $p < 0.05$).

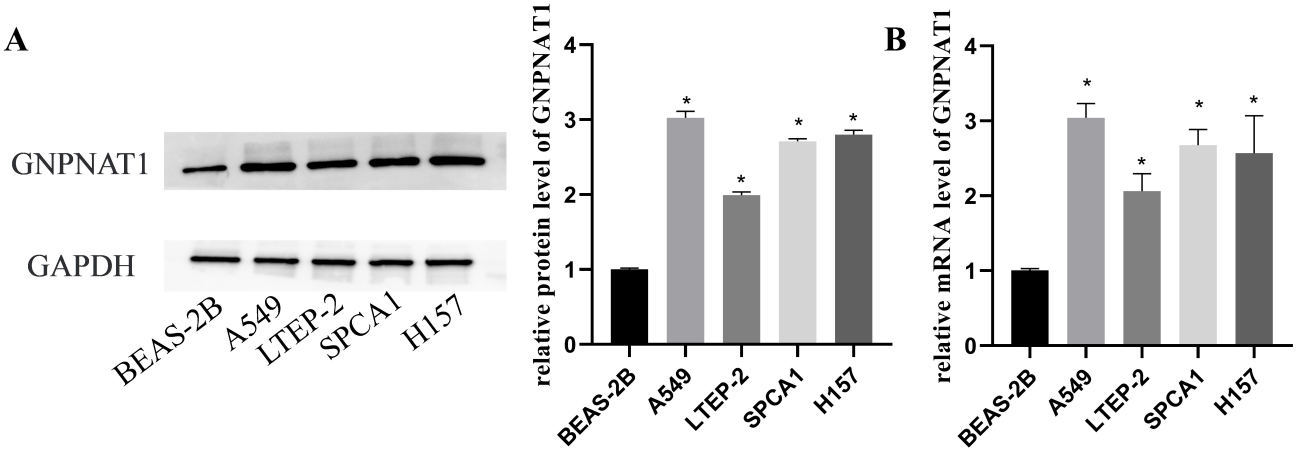

Fig. 2. GNPNAT1 was expressed in lung cancer cells. (A) Western blot detection of GNPNAT1 protein expression. (B) qRT-PCR detection of GNPNAT1 expression. * $p < 0.05$ vs. BEAS-2B. n = 3.

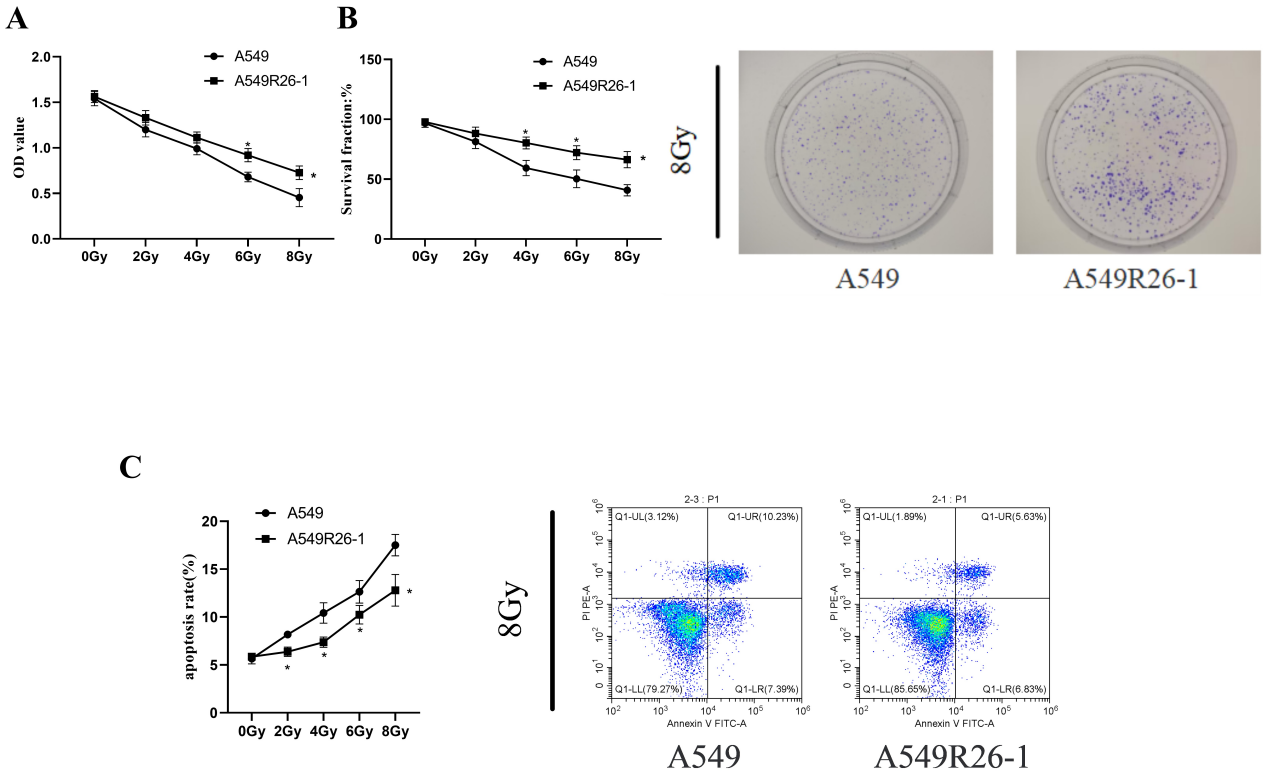

Fig. 3. Radioresistance of radioresistant lung cancer cells and parental cells. (A) Proliferative levels of radiation-resistant lung cancer cells and parental cells assessed by Cell Counting Kit-8 (CCK-8) assay. (B) Clonal levels of radiation-resistant lung cancer cells and parental cells determined by plate cloning assay. (C) Apoptosis levels in radiation-resistant lung cancer cells and parental cells measured by flow cytometry. * $p < 0.05$ vs. A549. n = 3. Gy, Gray.

Effect of GNPNAT1 on the Resistance to NK Cytotoxicity of Anti-Radiation Lung Cancer Cells

We evaluated the killing effect of NK cells on co-cultured A549R26-1 cells. The LDH release assay results indicated that the si-GNPNAT1-treated group showed increased sensitivity to NK cell cytotoxicity compared to the si-NC group. Conversely, A549R26-1 cells in the oe-GNPNAT1 group exhibited lower sensitivity to NK cell cytotoxicity compared to the oe-NC group. The NK cell co-culture colony formation assay further demonstrated that si-GNPNAT1 cells had significantly reduced colony formation compared to si-NC cells, whereas oe-GNPNAT1 cells

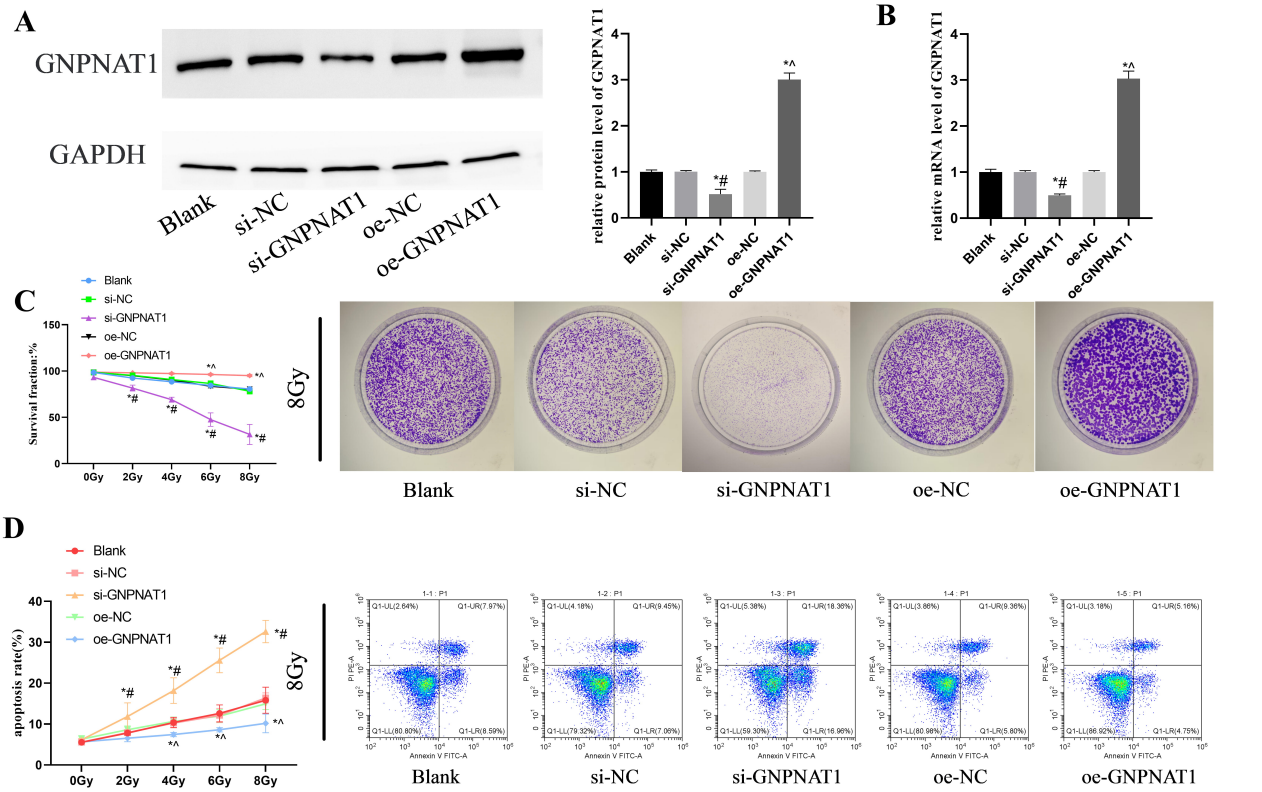

Fig. 4. Effect of GNPNAT1 on radioresistance of anti-radiation lung cancer cells. (A) Western blot detection of GNPNAT1 protein expression in A549R26-1 cells. (B) qRT-PCR detection of GNPNAT1 expression in A549R26-1 cells. (C) Cell viability in each group was assessed by plate cloning. (D) Apoptosis in each group was determined by flow cytometry. * $p < 0.05$ vs. Blank group. # $p < 0.05$ vs. si-NC. ^ $p < 0.05$ vs. oe-NC. n = 3.

exhibited significantly increased colony formation compared to oe-NC cells. These findings suggest that downregulation of GNPNAT1 expression enhances the sensitivity of radiation-resistant lung cancer cells to NK cell cytotoxicity (Fig. 5A,B, $p < 0.05$).

Discussion

Non-small cell lung cancer (NSCLC) is a prevalent malignancy worldwide, presenting significant therapeutic challenges [16]. Radiotherapy plays a crucial role in NSCLC treatment; however, the development of radioresistance limits its efficacy [17,18]. Despite the emergence of immunotherapy as a promising treatment modality for NSCLC, resistance remains a prevalent issue among patients [19,20]. Therefore, understanding the complex interplay between radioimmune function, the tumor microenvironment, and their underlying molecular mechanisms is critically important.

As a critical component of the immune system, natural killer (NK) cells play a pivotal role in mounting anti-tumor immune responses [21]. However, the tumor microenvironment often modulates and inhibits the cytotoxicity of NK cells against tumor cells [22]. Recent evidence highlights the involvement of intracellular molecular regulatory networks within tumor cells that influence NK cell activity [23], thereby affecting tumor immune evasion and therapeutic outcomes [24].

Therefore, investigating the intricate mechanisms and key molecules that govern NK cell cytotoxicity holds promise for understanding tumor immune tolerance mechanisms and developing novel immunotherapeutic strategies. This study aims to elucidate the role of GNPNAT1 in radioimmune function and NK cell cytotoxic resistance in NSCLC, with the goal of providing new insights and strategies to overcome immune tolerance in NSCLC.

This study investigated the role of GNPNAT1 in contributing to radioresistance in lung cancer, yielding significant findings. Initially, lung cancer patients were stratified, followed by experimental assessment, which revealed a substantial increase in GNPNAT1 expression in the radioresistant group compared to radiosensitive counterparts. Moreover, heightened GNPNAT1 expression was consistently observed across various lung cancer cell lines, particularly in A549 cells. These findings collectively indicate that GNPNAT1 plays a crucial role in the development and progression of lung cancer.

These findings are consistent with previous studies demonstrating the crucial role of GNPNAT1 in cancer cell proliferation and survival. Previous research has eluci-

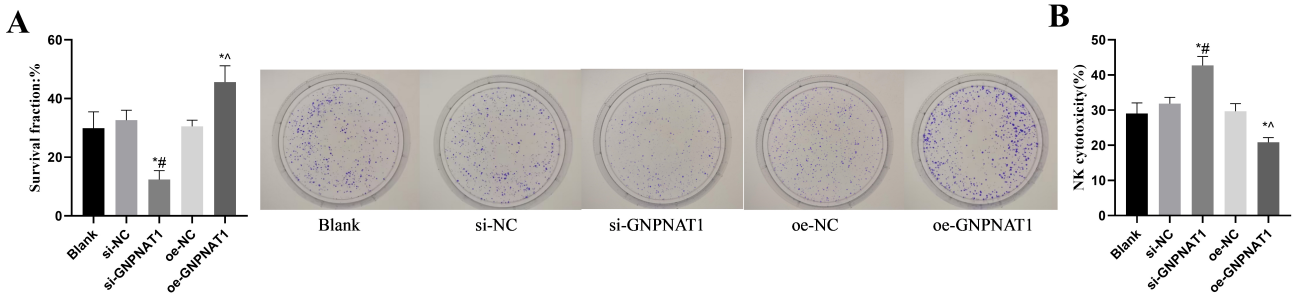

Fig. 5. Effect of GNPNAT1 on the resistance to NK cytotoxicity of anti-radiation lung cancer cells. (A) Cell viability in each group was assessed by plate cloning. (B) NK cell cytotoxicity against radiation-resistant lung cancer based on lactate dehydrogenase (LDH). * $p < 0.05$ vs. Blank group. # $p < 0.05$ vs. si-NC. ^ $p < 0.05$ vs. oe-NC. n = 3.

dated that GNPNAT1 participates in the biosynthesis of UDP-GlcNAc, a substrate essential for protein glycosylation, which is critical for cell signaling and tumor growth [25]. Our study expands on this knowledge by emphasizing GNPNAT1's specific involvement in mediating radioresistance in lung cancer.

Subsequent experiments revealed that radioresistant lung cancer cells (A549R26-1) exhibited increased proliferative and survival capacities, coupled with reduced apoptosis rates compared to parental cells (A549P), indicating heightened radioresistance. Manipulating GNPNAT1 expression levels showed that its downregulation mitigated radioresistance in these cells, while upregulation had the opposite effect. These findings underscore GNPNAT1's potential as a key regulator in mediating radioresistance in lung cancer.

Furthermore, the study found a correlation between NK cell cytotoxicity against radioresistant lung cancer cells and GNPNAT1 expression levels. Reduced GNPNAT1 expression enhanced the sensitivity of radioresistant lung cancer cells to NK cell cytotoxicity, whereas increased GNPNAT1 expression attenuated this sensitivity. These observations suggest GNPNAT1's potential role in modulating interactions between lung cancer cells and immune cells. Similar interactions have been reported in other study, further supporting GNPNAT1's involvement in the tumor microenvironment [26].

Despite these promising findings, our study has several limitations. Firstly, while our sample size was substantial, it may not fully represent all NSCLC patients, potentially limiting the generalizability of our results. Secondly, although A549 cell lines are commonly used in lung cancer research, they may not fully replicate the complexity of human tumors *in vivo* [27]. Future studies should include a broader range of cell lines and patient-derived xenograft models to validate our findings. Thirdly, our investigation primarily focused on GNPNAT1 expression at the protein and mRNA levels. Comprehensive analyses involving other regulatory mechanisms, such as epigenetic modifications and post-translational modifications, are needed to fully elucidate GNPNAT1's role in radioresistance [28].

Taken together, these findings underscore the significant role of GNPNAT1 in lung cancer radioresistance. Its expression levels appear to influence lung cancer cell proliferation, survival, and sensitivity to radiotherapy, while potentially modulating interactions between lung cancer cells and immune cells. These insights provide valuable directions for further investigation into the therapeutic potential of GNPNAT1 in lung cancer. Future research efforts could delve deeper into the molecular mechanisms underlying GNPNAT1 and its specific mode of action in lung cancer treatment, thereby offering novel targets and strategies for clinical interventions.

Conclusion

The downregulation of GNPNAT1 expression decreases immune resistance to radiotherapy in non-small cell lung cancer while increasing sensitivity to NK cell cytotoxicity.

Availability of Data and Materials

The data used and analyzed during the current study are available from the corresponding author.

Author Contributions

FX, YD and CY designed the research study. YD, CY, YL and WZ performed the research. FX, YL and JW provided help and advice on the experiments. WZ and JW analyzed the data. All authors were involved in the drafting and critical revision of the manuscript. All authors have read and approved the final manuscript. All authors have participated sufficiently in the work and agreed to be accountable for all aspects of the work.

Ethics Approval and Consent to Participate

This experiment has been approved by the ethics committee of The Affiliated Chuzhou Hospital of Anhui Medical University (CZH2023011). This study was conducted in strict accordance with the Declaration of Helsinki. All participants provided informed consent.

Acknowledgment

We would like to thank Gansu Cancer Hospital for their cooperation.

Funding

This research received no external funding.

Conflict of Interest

The authors declare no conflict of interest.

References

[1] Alexander M, Kim SY, Cheng H. Update 2020: Management of Non-Small Cell Lung Cancer. Lung. 2020; 198: 897–907.

[2] Mithoowani H, Febbraro M. Non-Small-Cell Lung Cancer in 2022: A Review for General Practitioners in Oncology. Current Oncology. 2022; 29: 1828–1839.

[3] Li Q, Zhang L, You W, Xu J, Dai J, Hua D, *et al*. PRDM1/BLIMP1 induces cancer immune evasion by modulating the USP22-SPI1-PD-L1 axis in hepatocellular carcinoma cells. Nature Communications. 2022; 13: 7677.

[4] Herbst RS, Morgensztern D, Boshoff C. The biology and management of non-small cell lung cancer. Nature. 2018; 553: 446–454.

[5] Pennell NA, Arcila ME, Gandara DR, West H. Biomarker Testing for Patients With Advanced Non-Small Cell Lung Cancer: Real-World Issues and Tough Choices. American Society of Clinical Oncology Educational Book. American Society of Clinical Oncology. Annual Meeting. 2019; 39: 531–542.

[6] Muthusamy B, Patil PD, Pennell NA. Perioperative Systemic Therapy for Resectable Non-Small Cell Lung Cancer. Journal of the National Comprehensive Cancer Network. 2022; 20: 953–961.

[7] Brown S, Banfill K, Aznar MC, Whitehurst P, Faivre Finn C. The evolving role of radiotherapy in non-small cell lung cancer. The British Journal of Radiology. 2019; 92: 20190524.

[8] Dohopolski M, Gottumukkala S, Gomez D, Iyengar P. Radiation Therapy in Non-Small-Cell Lung Cancer. Cold Spring Harbor Perspectives in Medicine. 2021; 11: a037713.

[9] Vecchiarelli S, Bennati C. Oncogene addicted non-small-cell lung cancer: current standard and hot topics. Future Oncology. 2018; 14: 3–17.

[10] Harada G, Gongora ABL, da Costa CM, Santini FC. TRK Inhibitors in Non-Small Cell Lung Cancer. Current Treatment Options in Oncology. 2020; 21: 39.

[11] Chen J, Wu F, Hou E, Zeng J, Li F, Gao H. Exosomal microRNA Therapy for Non-Small-Cell Lung Cancer. Technology in Cancer Research & Treatment. 2023; 22: 15330338231210731.

[12] Kaushik AK, Shojaie A, Panzitt K, Sonavane R, Venghatakrishnan H, Manikkam M, *et al*. Inhibition of the hexosamine biosynthetic pathway promotes castration-resistant prostate cancer. Nature Communications. 2016; 7: 11612.

[13] Tang A, Ahmad U, Toth AJ, Bourdakos N, Raja S, Raymond DP, *et al*. Non-small cell lung cancer in never- and ever-smokers: Is it the same disease? The Journal of Thoracic and Cardiovascular Surgery. 2021; 161: 1903–1917.e9.

[14] Dowling CM, Zhang H, Chonghaile TN, Wong KK. Shining a light on metabolic vulnerabilities in non-small cell lung cancer. Biochimica et Biophysica Acta. Reviews on Cancer. 2021; 1875: 188462.

[15] World Health Organization. WHO handbook for reporting results of cancer treatment. World Health Organization. 1979.

[16] Lu J, Han B. Liquid Biopsy Promotes Non-Small Cell Lung Cancer Precision Therapy. Technology in Cancer Research & Treatment. 2018; 17: 1533033818801809.

[17] Costa E Silva M, Silva E, Mendes A, Barroso A. Encephalitis in non-small-cell lung cancer. Pulmonology. 2021; 27: 582–583.

[18] He T, Cao J, Xu J, Lv W, Hu J. Minimally Invasive Therapies for Early Stage Non-small Cell Lung Cancer. Chinese Journal of Lung Cancer. 2020; 23: 479–486. (In Chinese)

[19] Pons-Tostivint E, Bennouna J. Treatments for Non-Small-Cell Lung Cancer: The Multiple Options for Precision Medicine. Current Oncology. 2022; 29: 7106–7108.

[20] J Saller J, Boyle TA. Molecular Pathology of Lung Cancer. Cold Spring Harbor Perspectives in Medicine. 2022; 12: a037812.

[21] Lee T, Clarke JM, Jain D, Ramalingam S, Vashistha V. Precision treatment for metastatic non-small cell lung cancer: A conceptual overview. Cleveland Clinic Journal of Medicine. 2021; 88: 117–127.

[22] Shih-Chun C, Shih-Chiang H, Chun-Yi T, Shan-Yu W, Keng-Hao L, Jun-Te H, *et al*. Non-small cell lung cancer with gastric metastasis and repeated gastrointestinal bleeding: A rare case report and literature review. Thoracic Cancer. 2021; 12: 560–563.

[23] Katzman D, Wu S, Sterman DH. Immunological Aspects of Cryoablation of Non-Small Cell Lung Cancer: A Comprehensive Review. Journal of Thoracic Oncology. 2018; 13: 624–635.

[24] VanderLaan PA, Roy-Chowdhuri S. Current and future trends in non-small cell lung cancer biomarker testing: The American experience. Cancer Cytopathology. 2020; 128: 629–636.

[25] Hascall VC, Wang A, Tammi M, Oikari S, Tammi R, Passi A, *et al*. The dynamic metabolism of hyaluronan regulates the cytosolic concentration of UDP-GlcNAc. Matrix Biology. 2014; 35: 14–17.

[26] Efimova I, Catanzaro E, Van der Meeren L, Turubanova VD, Hammad H, Mishchenko TA, *et al*. Vaccination with early ferroptotic cancer cells induces efficient antitumor immunity. Journal for Immunotherapy of Cancer. 2020; 8: e001369.

[27] McCafferty S, Haque AKMA, Vandierendonck A, Weidensee B, Plovyt M, Stuchlíková M, *et al*. A dual-antigen self-amplifying RNA SARS-CoV-2 vaccine induces potent humoral and cellular immune responses and protects against SARS-CoV-2 variants through T cell-mediated immunity. Molecular Therapy. 2022; 30: 2968–2983.

[28] Yam-Puc JC, Hosseini Z, Horner EC, Gerber PP, Beristain-Covarrubias N, Hughes R, *et al*. Age-associated B cells predict impaired humoral immunity after COVID-19 vaccination in patients receiving immune checkpoint blockade. Nature Communications. 2023; 14: 3292.